Archives of Photogrammetry, Cartography and Remote Sensing, vol. 35, pp. 107-124
ISSN 2083-2214, eISSN 2391-9477
DOI: http://doi.org/10.14681/apcrs-2023-005

RESEARCH ARTICLE

THE USE OF DIFFERENT MEASUREMENT TECHNOLOGIES TO CALCULATE THE VOLUME OF A ROCK OBJECT IN THE WIETRZNIA NATURE RESERVE IN KIELCE

Artur Warchoł, Łukasz Kapusta, Karolina Cieciora, Filip Grzyb, Marcin Walski

Department of Geodesy and Geomatics, Faculty of Environmental Engineering, Geomatics and Renewable Energy, Kielce University of Technology

KEY WORDS: volume calculation, rock object, GNSS-RTK method, laser scanning, LiDAR, reference level

ABSTRACT: The paper presents a procedure for measuring the volume of an atypical object with an irregular shape, which is a rock formation located in the Wietrznia Nature Reserve in Kielce. Two measurement techniques were used: GNSS-RTK and terrestrial laser scanning. The use of independent measurement technologies allowed comparison of the results obtained. The results obtained lead to a discussion on the influence of the density of measurement points on the quality of the obtained results. On the basis of the measurements made, it is also possible to assess the labour intensity of the solutions applied.

1. INTRODUCTION

Nowadays it is easier than ever to create data, especially digital data. In a large number of cases these are geospatial data. On the one hand, it is good that we have more collections to conduct research (Apollo *et al.*, 2023), while on the other hand there is a danger of getting lost in such a large amount of them (Gawronek & Noszczyk, 2023; Wadowska *et al.*, 2022). Data with a spatial attribute is used in a great many fields both at the macro scale - country, region, city, or at the micro scale - object, building. Examples at the macro scale include studies on noise (Szopińska *et al.*, 2022), urban development (Balawejder *et al.*, 2018; Krajewska *et al.*, 2021), the property market (Buśko *et al.*, 2022; Cienciała *et al.*, 2023), the promotion of tourist attractions (Bieda *et al.*, 2021; Gorgoglione *et al.*, 2023), documentation of natural disaster sites (Toni *et al.*, 2023), air pollution (Szopińska *et al.*, 2022), land consolidation process (Basista *et al.*, 2023) and effects of land consolidation (Balawejder *et al.*, 2021). At the micro scale, examples of the use of spatial data can be found, among others, for the creation of digital documentation of heritage objects (Pastucha *et al.*, 2018), acquisition of the geometry of a historic bell (Skrzypczak *et al.*, 2023), building thermal inspection (Stokowiec & Sobura, 2023) or monitoring of flood protection objects (Kurczyński & Bakuła, 2016).

LiDAR technology itself is used on a large scale in different solutions and from different ceilings: aerial (ALS - Airborne Laser Scanning) - e.g. (Kurczyński & Bakuła 2013; Zapłata *et al.*, 2018; Lisańczuk *et al.*, 2020; Janus *et al.*, 2021), ULS - UAV-borne Laser Scanning (Di Stefano *et al.*, 2023; Yang & Li, 2022; Bakuła *et al.*, 2020), MLS - Mobile Laser Scanning (Di Stefano *et al.*, 2021; Wang *et al.*, 2020) or TLS - Terrestrial Laser Scanning.

We can find examples of the application of Terrestrial Laser Scanning (TLS) technology in many publications. These may relate to accuracy considerations (Warchoł, 2015), optimisation (Błaszczak-Bąk *et al.*, 2022), hazardous area monitoring (Zhao *et al.*, 2022; Weidner & Walton 2021), inventory (Sobura *et al.*, 2023; Gawronek *et al.*, 2017), inspection (Wolski *et al.*, 2022), data integration (Klapa *et al.*, 2017; Liu *et al.*, 2023; Warchoł *et al.*, 2016) and model creation for BIM (Skrzypczak *et al.*, 2022; Warchoł & Lęcznar in Wolski 2022; Warchoł 2019).

One of the fundamental problems accompanying volume measurements of existing objects is the optimal definition of two types of surfaces enclosing the solid under analysis. These are:

- theoretical surfaces - "bottom", set by the designer or resulting from certain conditions, (defined for calculation purposes),
- topographic surfaces - "upper", inventoried on the basis of field measurements.

The topographic surface delimiting the surveyed solid is usually covered from above with a grid of points where the measurement is carried out. The choice of the shape of the grid (TIN or GRID) and the density of points covering the topographic surface depends on many factors, including the complexity of the shape of the surveyed object or its availability for measurement (Szczepaniak-Kołtun, 2016). The set of points representing the surface defining the solid under study forms the basis for dividing the solid into elementary prisms with a triangular (TIN) or square (GRID) base. The volume of the whole is equal to the sum of the volumes of the elementary solids:

$$V = \sum_{i=1}^{n} V_i \tag{1}$$

where:

V - total volume of the solid,

Vi - volume of the i-th elementary solid.

A schematic sketch of an elementary solid with a triangular base is presented in Figure 1.

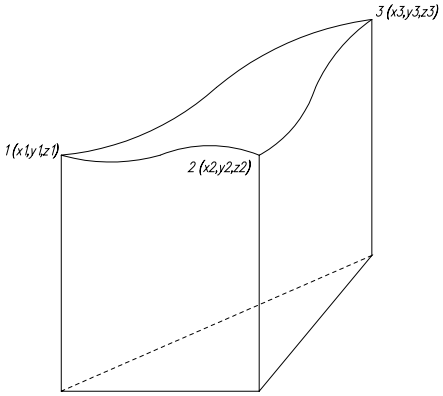

Fig. 1 An elementary solid with a triangular base (source: own elaboration)

The volume of an elementary solid is expressed by the formula:

$$V = \frac{1}{3}P(z_1 + z_2 + z_3) \tag{2}$$

where:
z_1, z_2, z_3 - level difference between the bounding surfaces at points: 1, 2 and 3,
P - area of the base of the solid (triangle) determined from the formula:

$$P = \frac{1}{2}\begin{vmatrix} \Delta x_{12} & \Delta y_{12} \\ \Delta x_{13} & \Delta y_{13} \end{vmatrix} \tag{3}$$

where:
$\Delta x, \Delta y$ - difference of plane coordinates for selected pairs of points/sides of the triangle.

A common and widely used measurement technique for acquiring the shape of a topographic surface today is GNSS-RTK technology. With it, real-time measurements can easily be taken. The results obtained, the x,y,z coordinates, form the basis for further calculations. Two points are worth mentioning at this point. The first is the choice of grid density. An ill-advised measurement, lacking intuition on the part of the surveyor, can have a significant impact on the results obtained. For example, when defining the vertical cross-section of an object to be measured, all points relevant to the results obtained should be included in the measurements. In Figure 2, the red colour represents the cross-section generated from the measurement at points:1-4. The black colour represents the actual cross-section.

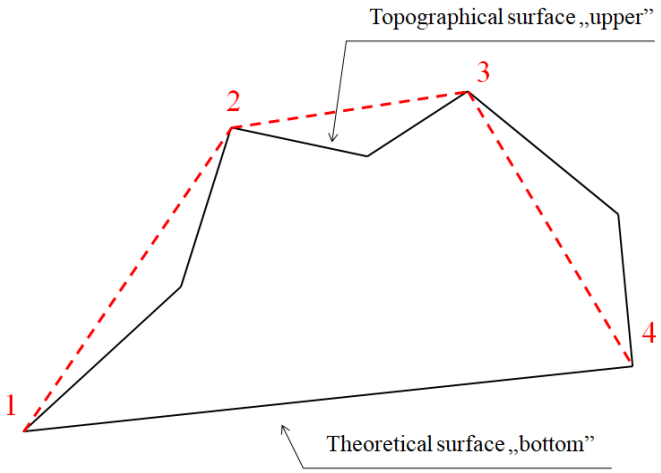

Fig. 2. Impact of the surveyor's selection of measurement points - vertical cross-section. Black line - actual shape of the terrain, red line - terrain relief resulting from selection of points 1-4 by the surveyor as measurement points characterizing the shape of the object.

Omission of the selected characteristic points of the cross-section in the measurements results in lowering the accuracy of the obtained result. The second issue to be addressed here is the availability of the measurement object. In order to carry out GNSS-RTK measurements at all characteristic points, it is first necessary to reach them. This can prove difficult in practice.

An alternative to GNSS-RTK measurements is terrestrial laser scanning (TLS - Terrestrial Laser Scanning). Firstly, the scanning technique allows measurements on objects that are difficult to access. The measurement itself generally does not require entry to the object. Secondly, the scanning process produces an extensive data set in the form of point clouds. The measured object is covered by a dense grid of measurement points. In contrast, the procedure itself for processing laser scanning data is more complicated due to the amount of data and problems of interpretation.

The issue of creating a Digital Terrain Model (DTM) has been around for a long time. Firstly created using aerial photographs, topographic maps or direct measurements - total station or GNSS (Hejmanowska & Warchoł 2011) and finally based on LiDAR datasets (Biszof & Oberski, 2018; Warchoł, 2013; Bakuła, 2023) or SfM (Salach *et al.*, 2018). Important aspects are both the survey work and the ways of data processing and reduction of redundant data in DTM collections (Bakuła & Kurczyński 2013; Bakuła *et al.*, 2013). Comparisons of results depending on the key aspects can be found e.g.: (Poręba, 2009) - obtained with different measurement methods or in (Warchoł *et al.*, 2019) - different measurement technologies and different calculation software.

2. RESEARCH OBJECT

The aim of this study is to compare the measurement techniques used in the acquisition of points representing a topographic surface. The object under measurement is a rock

formation located within the Zbigniew Rubinowski Wietrznia Nature Reserve in Kielce. This is an inanimate nature reserve located in the south-eastern part of Kielce. It consists of three interconnected former quarries: Wietrznia, Międzygórz and Międzygórz Wschodni built from Upper Devonian limestone and dolomite rocks. The quarry was created as a result of exploitation of the deposit in the years 1893 - 1974.

The rock formation included in the measurement is located in the central part of the Międzygórz quarry. In shape, it resembles a cone with an irregular surface. The horizontal dimensions of the object are approximately: base 50×30m, height 14 metres. The object is covered in a small part by grass vegetation and sparse shrubs (Figure 3).

Fig. 3. Inventoried rock object
(Source: https://geopark.pl/rezerwat-wietrznia/)

3. DATA AQUSITION

Measurements used survey techniques commonly used today for topographic data acquisition:

- measurement using GNSS-RTK technology,
- data acquisition with a scanning total station,
- performing LiDAR terrestrial laser scanning.

GNSS-RTK measurements were performed using the Sokkia kit: GRX1 receiver and SHC-250 controller. Sokkia GRX1. Scanning was performed with a Topcon QS1A robotic total station with scanning option and a Faro Focus S150 scanner.

First, the survey network around the surveyed object was stabilised. GNSS-RTK measurements at all 9 points of the stabilised network (Figure 4) were carried out in three measurement series with the final coordinates averaged.

Fig. 4. Sketch of the established survey network
(source: own elaboration)

The next step was to measure points on the object using the GNSS-RTK technique. First, the outline of the lower base of the test object was defined: a total of 23 points connected by the green broken line in Figure 5. Next, the geometry of the shape of the topographic surface bounding the test volume from above was measured. It is represented by points located in the characteristic places of the test object and at the same time inside the previously measured contour (a total of 29 points - Figure 5). The next measurement step was scanning of zones difficult to access for direct measurements, such as the rocky north wall of the object visible in the central part in Figure 5. As a result of scanning with a scanning total station from the points of the surveying network, several hundred additional points representing the topographic surface of the surveyed object were obtained. Figure 5 summarises the location of the GNSS-RTK measured points (left side), and the GNSS-RTK + selected total station scan points (right side), based on which the volume calculations realised in the spreadsheet were performed.

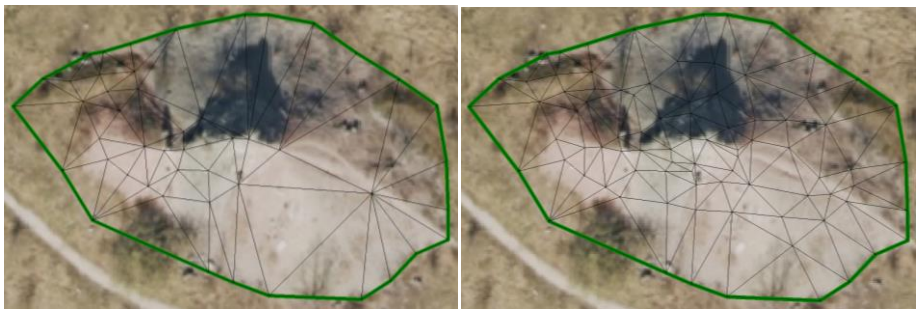

Fig. 5. Inventoried object with triangular grid; left: GNSS-RTK, right: GNSS-RTK + total station scanning (source: own elaboration)

TLS LiDAR using a Faro Focus s150 scanner began with preparatory work. Prior to the survey, a field interview was carried out and the number of scanner positions necessary for proper site data collection was determined. The locations of the stabilised reference points - black and white targets, nails and wooden stakes - were also planned. Figure 6 shows in red the scanner stations and in yellow and blue the nails/stakes and targets that are the control points, respectively. The stakes and nails were stabilised interchangeably, depending on the substrate at the planned location of the point.

Fig. 6. Plan of scanner positions and stabilisation of reference points (source: own elaboration)

Once the positions were planned and the points stabilised, the scanner was sequentially positioned at the survey stations taking scans. The scanning resolution was set at - points every 6.1 mm at a distance of 10 m from the scanner. Spheres (Figure 7) were used to later connect the scans by positioning them in the field in such a way that they were visible on adjacent scans.

Fig. 7: Spheres used for registration of the TLS scans

4. RESULTS

In order to make an initial estimate of the volume of the surveyed shape, a representative group of points approximately evenly distributed over the height of the object was selected from the point cloud obtained from the scanning total station measurement. Data selection at this stage effectively reduced the calculation algorithm built in the spreadsheet. The set of results obtained from the GNSS-RTK measurement was then added to the analysed results. For the data set prepared in this way, representing the topographic surface, a subdivision was made into prisms with a triangular base (Figure 8).

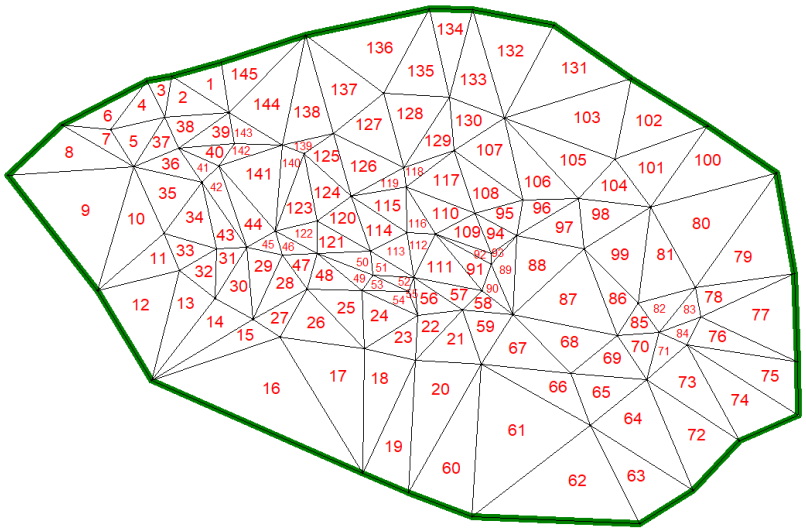

Fig. 8 Division of the solid into elementary prisms

In defining the area enclosing the surveyed volume from below, the results of measuring the object's base contour using GNSS-RTK were used. In the calculation algorithm used in Excel, the bottom-enclosing surface is a plane whose angle of inclination was calculated on the basis of approximation after the base contour points were projected onto a vertical plane running along the maximum overall dimension of the surveyed object (Figure 9).

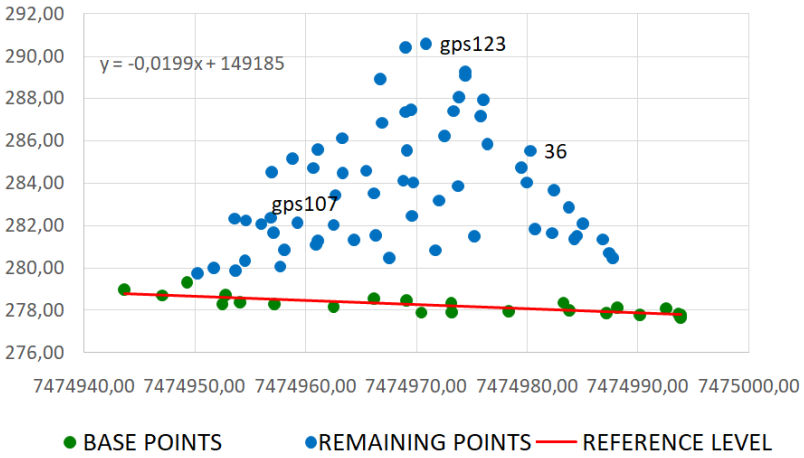

Fig. 9. Trend line with points above the reference level (source: own elaboration)

Using the algorithm presented in the introduction - formulas (1) and (2), the volumes of the elementary prisms were calculated in Excel. The total volume of the studied object is 3823 m^3.

Analogous calculations were made based only on the results of the GNSS-RTK measurements, omitting the previously selected points obtained from the total station scanning process. The diluted grid representing the individual bases of the elementary prisms is shown in Figure 10.

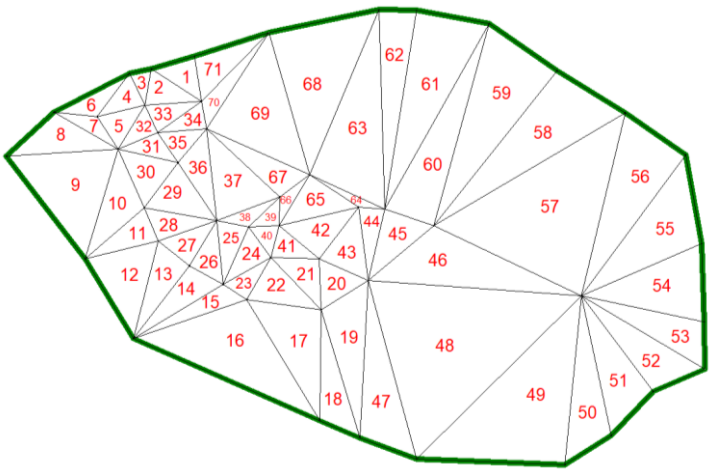

Fig. 10. Partitioning into elementary solids on the basis of GNSS-RTK measurements

The volume from the calculation in Excel software obtained solely on the basis of the GNSS-RTK measurements is 3730 m^3.

In the second calculation step, the WinKalk software commonly used in surveying practice was used to calculate the volume on the basis of GNSS-RTK and GNSS-RTK + scanning total station measurements. The calculations were performed for the same reduced number of points representing the topographic surface of the surveyed object. This approach made sense in the context of later comparing the results from the two calculation attempts: Excel and WinKalk. With a much larger number of data, calculations in Excel would have been cumbersome. On the other hand, the definition of the topographic surface based on the set of data obtained from the scanning total station would have been different to that adopted in Excel. The WinKalk software performs volume calculations starting by connecting points into a triangular grid (Figure 11).

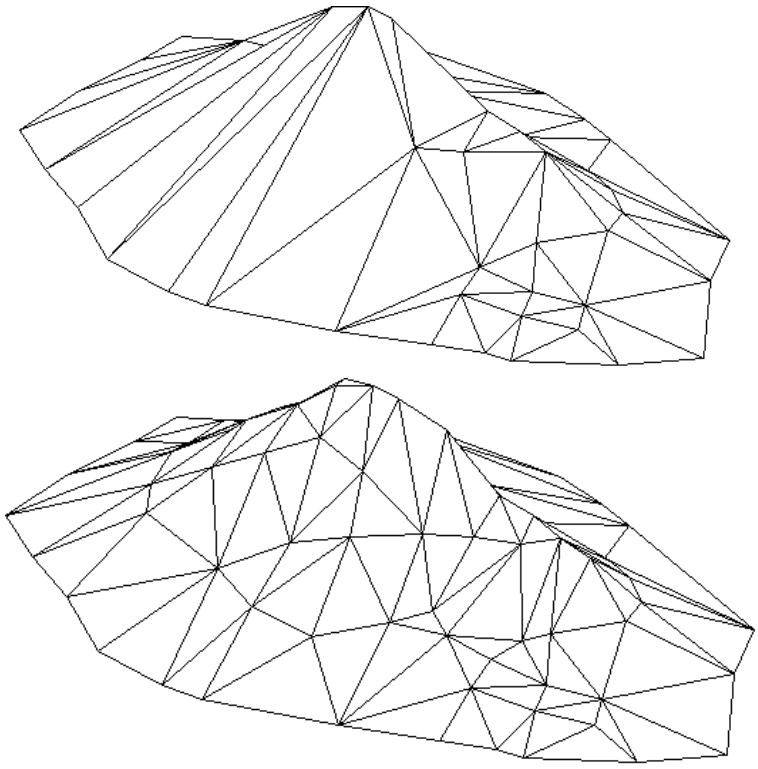

Fig. 11. Comparison of the 3D model generated in WinKalk; top: GNSS-RTK, bottom: GNSS-RTK + total station laser scanning (source: own elaboration)

Then, for each triangle formed, it calculates the volume of the prism from a fixed reference level, up to the height of the triangle vertices, according to the notation presented in the introduction of the work. The results obtained are respectively: 3776 m^3 for GNSS-RTK + total station scanning and 3679 m^3 GNSS-RTK.

The slight differences in the results (approx. 1%) obtained with the Winkalk software and those obtained in Excel may be due to the fact that the basal area enclosing the surveyed mass from below is defined differently. Figure 12 shows the surface area in question generated based on the perimeter points in the Winkalk software.

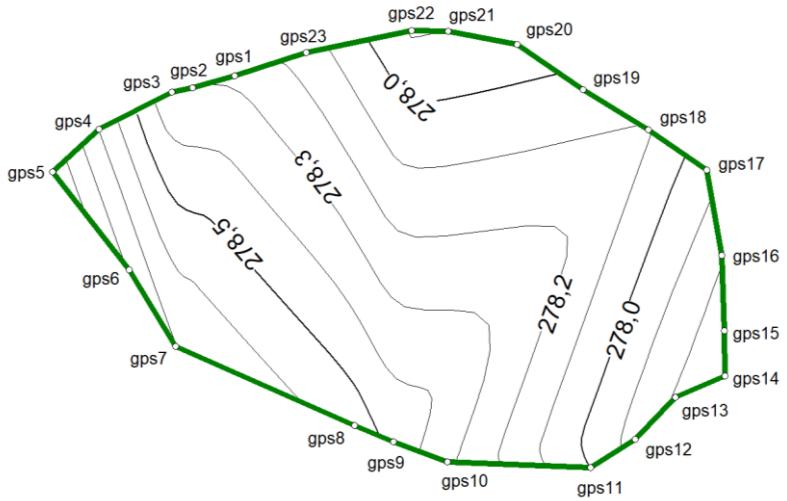

Fig. 12. Contour map of the base of the study site - bottom surface.

However, the results from both computational approaches are very close (a difference of about 1%), which practically excludes the occurrence of a coarse error in the results obtained.

The calculation of the volume of the same rock formation, but based on a much more detailed measurement made with the Faro Focus s150 scanner, was developed in a similar way. Trimble Business Centre software was used. A combined point cloud representing the topographic surface bounding the surveyed rock formation from above was exported from Trimble RealWorks to .las format. These files were then uploaded into Trimble Business Center software for further calculations. Before starting the volume calculations, the point cloud was cleaned. Elements such as scanned trees and shrubs overgrowing the rock formation under study were removed. The final product of the cleaned cloud consists of 62 280 450 points (Figure 13).

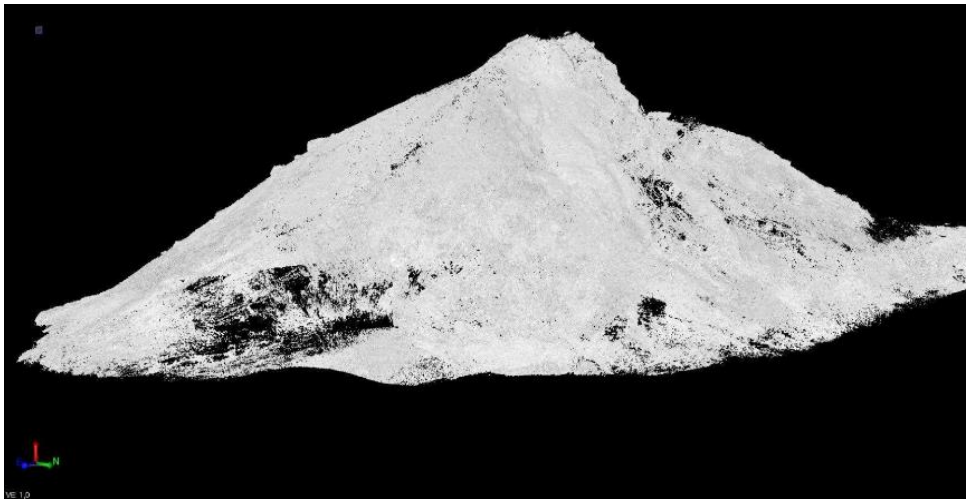

Fig. 13. Point cloud acquired from scanning with Faro Focus s150 scanner after cleaning

The Trimble Business Center software allows the volume to be calculated according to the same principle used to develop the GNSS-RTK results. As in WinKalk, the volume is determined in the Trimble software in the option: "surface to surface". The top surface in the calculation was, in this case, a model based on a point cloud. Importantly, the bottom surface was defined here identically to the first case. It was built on the basis of the contour measured by the GNSS-RTK technique (Figure 8 - green polyline).

The largest volume value was obtained from the Faro Focus s150 scanner measurement (Table 1). The smallest volume is that obtained from GNSS-RTK measurements. The differences are small. Between the GNSS-RTK results and the scan made with the Faro Focus s150 scanner, the difference is 123 m3 which is 3.3% of the surveyed volume.

Table 1. Summarises of the calculated volumes and the labour intensity of the different measurement methods.

	GNSS-RTK	GNSS-RTK + total station scanning	TLS Faro Focus s150
Number of points	48	85	62 280 450
Volume in m^3	3679	3776	3802
Time for field work	1 h	2 h	9 h
Postprocessing time	-	1 h	3 h

The GNSS-RTK volume result supplemented by the scanning total station is already very close to the results obtained from the point cloud from the scanning with the scanner. A total of 26 m^3 of difference represents less than 1%. It is worth mentioning that the topographic surface defining the calculated volume in the GNSS-RTK + scanning total station measurement is represented in the task by less than 100 points, while the same surface from the Faro scan is built on a cloud of more than 62 million points.

5. CONCLUSIONS

Topographic surface shape measurements using GNSS-RTK provide an effective solution in acquiring data for volume calculations. It is not a major problem to carry out this type of measurement, provided that the object to be surveyed is accessible. However, the more complex the shape of the object, the more difficult it is to inventory its surface with high accuracy. Then a GNSS-RTK measurement may not be sufficient. An alternative to such GNSS-RTK measurements is LiDAR terrestrial laser scanning. The measurement procedure itself is more complex. In addition, the results obtained are more difficult to interpret. In order to successfully calculate the volume based on the topographic surface, the scans must first be cleaned.

As the obtained results showed, with the process of densification of points covering the surveyed object, the obtained result is more and more precise. It is worth noting that correctly planned and carried out GNSS-RTK measurements on only about 50 points allowed to obtain similar results of the surveyed volume as in the case of a point cloud of over 62 million points scanned with high resolution. This indicates in this case the high redundancy of the acquired data. Terrestrial laser scanning technology, on the other hand, would undoubtedly be difficult to replace by GNSS-RTK when measuring structures with a much more complex shape or for inaccessible sites where the surveyor has not been granted access.

LITERATURE

Apollo, M., Jakubiak, M., Nistor, S., Lewinska, P., Krawczyk, A., Borowski, Ł., Specht, M., Krzykowska-Piotrowska, K., Marchel, Ł., Pęska-Siwik, A., Kardoš, M., Maciuk, K. 2023. Geodata in science—A review of selected scientific fields, *Acta Sci. Pol. Form. Circumiectus*, 22, 17–40. https://doi.org/10.15576/ASP.FC/2023.22.2.02.

Bakuła, K., Pilarska, M., Ostrowski, W., Nowicki, A., & Kurczyński, Z. 2020. UAV LiDAR data processing: influence of flight height on geometric accuracy, radiometric information and parameter setting in DTM production, *Int. Arch. Photogramm. Remote Sens. Spatial Inf. Sci.*, XLIII-B1-2020, 21–26, https://doi.org/10.5194/isprs-archives-XLIII-B1-2020-21-2020.

Bakuła, K., Kurczyński, Z. 2013. The role of structural lines extraction from high-resolution digital terrain models in the process of height data reduction, *13th SGEM GeoConference on Informatics, Geoinformatics and Remote Sensing*, 579-586.

Bakuła, K., Olszewski, R., Bujak, Ł., Gnat, M., Kietlińska, E., Stankiewicz, M. 2013. Generalizacja NMT w opracowaniu metodologii reprezentacji rzeźby terenu. *Archives of Photogrammetry, Cartography and Remote Sensing*, 25, 19-32.

Bakuła, K., 2023. Accuracy of digital elevation models obtained from unmanned laser scanning data in the era of ULS technology development. *Przegląd Geodezyjny*, 95(9), http://dx.doi.org/0000-0001-7137-1667.

Balawejder M., Matkowska K., Çolak H.E., 2018. The Impact of Surveying Works on the Development of Smart City. *Geographic Information Systems Conference and Exhibition "GIS ODYSSEY 2018"*, Conference Proceedings, Italy 10th to 14th of September 2018, Perugia, https://depot.ceon.pl/handle/123456789/16173.

Balawejder M., Matkowska K., Rymarczyk E., 2021. Effects of land consolidation in Southern Poland. *Acta Scientiarum Polonorum Administratio Locorum* 20 (4), 269-282 https://www.ceeol.com/search/article-detail?id=1018076.

Basista I., Balawejder M., Kuchta A. 2023. A land consolidation geoportal as a useful tool in land consolidation projects – A case study of villages in southern Poland. *Acta Scientiarum Polonorum Administratio Locorum*, 22(4), 453–469. https://doi.org/10.31648/aspal.9250.

Bieda A., Balawejder M., Warchoł A., Bydłosz J., Kolodiy P., Pukanská K. 2021. Use of 3d technology in underground tourism: Example of Rzeszow (Poland) and Lviv (Ukraine). *Acta Montanistica Slovaca*, 26 (26), 205–21. DOI: https://doi.org/10.46544/ams.v26i2.03.

Biszof, A., Oberski, T., 2018. Możliwości generowania precyzyjnego NMT na podstawie chmury punktów z projektu ISOK. *Archives of Photogrammetry, Cartography and Remote Sensing*, 30, 95-106.

Błaszczak-Bąk W., Suchocki C., Mrówczyńska M. 2022. Optimization of Point Clouds for 3D Bas-Relief Modeling. *Autom. Constr.*, 140, 104352. https://doi.org/10.1016/j.autcon.2022.104352.

Buśko M., Zyga J., Hudecová Ľ., Kyseľ P., Balawejder M., Apollo M. 2022. Active Collection of Data in the Real Estate Cadastre in Systems with a Different Pedigree and a Different Way of Building Development: Learning from Poland and Slovakia. *Sustainability*; 14(22), 15046. https://doi.org/10.3390/su142215046.

Cienciała A., Sajnóg N., Sobolewska-Mikulska K., 2023. Unreliability of cadastral data on parcel area and its effect on sustainable real estate valuation. *Reports on Geodesy and Geoinformatics* 116 (1), 39-46. 10.2478/rgg-2023-0009.

Di Stefano F., Chiappini S., Gorreja A., Balestra M., Pierdicca R., 2021. Mobile 3D scan LiDAR: a literature review, *Geomatics, Natural Hazards and Risk*, 12:1, 2387-2429, DOI: 10.1080/19475705.2021.1964617.

Di Stefano F., Pierdicca R., Malinverni E. S., Corneli A., & Naticchia B. 2023. Point cloud classification of an urban environment using a semi-automatic approach, *Int. Arch. Photogramm. Remote Sens. Spatial Inf. Sci.*, XLVIII-1/W1-2023, 131–138, https://doi.org/10.5194/isprs-archives-XLVIII-1-W1-2023-131-2023, 2023.

Gawronek P., Makuch M., Mitka B., Bożek P., Klapa P. 2017. 3D Scanning of the Historical Underground of Benedictine Abbey in Tyniec (Poland). In *Proceedings of the International Multidisciplinary Scientific GeoConference: SGEM-Section Geodesy and Mine Surveying*, Albena, Bulgaria, 29 June–5 July 2017. https://doi.org/10.5593/sgem2017/22.

Gawronek P., Noszczyk T. 2023. Does more mean better? Remote-sensing data for monitoring sustainable redevelopment of a historical granary in Mydlniki, Kraków. *Herit Sci.* 11, 23 (2023). https://doi.org/10.1186/s40494-023-00864-0

Gorgoglione L., Malinverni E.S., Smaniotto Costa C., Pierdicca R., Di Stefano F. 2023. Exploiting 2D/3D Geomatics Data for the Management, Promotion, and Valorization of Underground Built Heritage. *Smart Cities* 2023, 6, 243-262. https://doi.org/10.3390/smartcities6010012.

Hejmanowska B., Warchoł A. 2011. Analiza porównawcza wysokości terenu uzyskanej za pomocą lotniczego skaningu laserowego, pomiaru GPS oraz pomiaru na modelu stereoskopowym z kamery ADS 40, *Acta Scientiarum Polonorum. Geodesia et Descriptio Terrarum* 9 (3), 13-24.

Janus J., Bożek P., Mitka B., Taszakowski J., Doroż A., 2021. Long-term forest cover and height changes on abandoned agricultural land: An assessment based on historical stereometric images and airborne laser scanning data. *Ecological Indicators*, 120, 106904, https://doi.org/10.1016/j.ecolind.2020.106904.

Klapa P., Mitka B., Zygmunt M. 2017. Application of Integrated Photogrammetric and Terrestrial Laser Scanning Data to Cultural Heritage Surveying. *IOP Conf. Ser.: Earth Environ.* Sci. 95 032007.

Krajewska M., Szopińska K., Siemińska E., 2021. Value of land properties in the context of planning conditions risk on the example of the suburban zone of a Polish city. *Land Use Policy*, 109, 105697, https://doi.org/10.1016/j.landusepol.2021.105697.

Kurczyński, Z. Bakuła, K., 2013. Generowanie referencyjnego numerycznego modelu terenu o zasięgu krajowym w oparciu o lotnicze skanowanie laserowe w projekcie ISOK. *Archives of Photogrammetry, Cartography and Remote Sensing*, 59-68.

Kurczyński, Z. Bakuła, K., 2016. SAFEDAM-zaawansowane technologie wspomagające przeciwdziałanie zagrożeniom związanym z powodziami. *Archives of Photogrammetry, Cartography and Remote Sensing*, 28, 39-52.

Lisańczuk M., Mitelsztedt K., Parkitna K. *et al.*, 2020. Influence of sampling intensity on performance of two-phase forest inventory using airborne laser scanning. *For. Ecosyst.* 7, 65 . https://doi.org/10.1186/s40663-020-00277-6.

Liu J, Willkens D, Gentry R. A. 2023. Conceptual Framework for Integrating Terrestrial Laser Scanning (TLS) into the Historic American Buildings Survey (HABS). *Architecture*; 3(3), 505-527. https://doi.org/10.3390/architecture3030028.

Pastucha E., Rzonca A., Szombara S. 2018. Digital Documentation of Heritage Objects on Non-Developable Surfaces, *2018 Baltic Geodetic Congress (BGC Geomatics)*, Olsztyn, Poland, 159-163, doi: 10.1109/BGC-Geomatics.2018.00036.

Poręba M., 2009. Modern methods of earth mass volume determination. *Archives of Photogrammetry, Cartography and Remote Sensing*, 19, 351-361, Kraków.

Salach A, Bakuła K, Pilarska M, Ostrowski W, Górski K, Kurczyński Z. 2018. Accuracy Assessment of Point Clouds from LiDAR and Dense Image Matching Acquired Using the UAV Platform for DTM Creation. *ISPRS International Journal of Geo-Information*; 7(9),342. https://doi.org/10.3390/ijgi7090342.

Skrzypczak I., Oleniacz G., Leśniak A., Zima K., Mrówczyńska M., Kazak J.K.. 2022. Scan-to-BIM Method in Construction: Assessment of the 3D Buildings Model Accuracy in Terms Inventory Measurements. *Build. Res. Inf.*, 50, 859–880. https://doi.org/10.1080/09613218.2021.2011703.

Skrzypczak I., Oleniacz G., Leśniak A. *et al.*, 2023. A practical hybrid approach to the problem of surveying a working historical bell considering innovative measurement methods. *Herit Sci.* 11, 152. https://doi.org/10.1186/s40494-023-01007-1.

Sobura S., Bacharz K., Granek G. 2023. Analysis of Two-Option Integration of Unmanned Aerial Vehicle and Terrestrial Laser Scanning Data for Historical Architecture Inventory. *Geod. Cartogr*., 49, 76–87. https://doi.org/10.3846/gac.2023.16990.

Stokowiec K., Sobura S. 2023 Building thermal inspection case study - Appropriability assessment of hand-held and UAV infrared camera. *AIP Conf. Proc*. 27 November 2023; 2847 (1): 050010. https://doi.org/10.1063/5.0166021.

Szczepaniak-Kołtun Z. 2016. Assessment of DTM resolution influence on the accuracy of flow lines extraction. *Archives of Photogrammetry, Cartography and Remote Sensing*. 28, 115-124. DOI: 10.14681/afkit.2016.009.

Szopińska K., Balawejder M., Warchoł A., 2022. National legal regulations and location of noise barriers along the Polish highway. *Transportation Research Part D: Transport and Environment*, 109, 103359, https://doi.org/10.1016/j.trd.2022.103359.

Szopińska K, Cienciała A, Bieda A, Kwiecień J, Kulesza Ł, Parzych P. 2022. Verification of the Perception of the Local Community concerning Air Quality Using ADMS-Roads Modeling. *International Journal of Environmental Research and Public Health*.; 19(17):10908. https://doi.org/10.3390/ijerph191710908.

Tonti I, Lingua AM, Piccinini F, Pierdicca R, Malinverni ES. 2023. Digitalization and Spatial Documentation of Post-Earthquake Temporary Housing in Central Italy: An Integrated Geomatic Approach Involving UAV and a GIS-Based System. *Drones*.; 7(7):438. https://doi.org/10.3390/drones7070438.

Wadowska A, Pęska-Siwik A, Maciuk K. 2022. Problems of collecting, processing and sharing geospatial data. *Acta Scientiarum Polonorum. Formatio Circumiectus*.;21(3-4), 5-16. doi:10.15576/ASP.FC/2022.21.3/4.5.

Wang C., Wen C., Dai Y., Yu S., Liu M. 2020. Urban 3D modeling using mobile laser scanning: a review. *Virtual Reality & Intelligent Hardware*. Volume 2, Issue 3, 175-212, https://doi.org/10.1016/j.vrih.2020.05.003.

Warchoł A., 2013. Analiza dokładności przestrzennej danych z lotniczego, naziemnego i mobilnego skaningu laserowego jako wstęp do ich integracji. *Archives of Photogrammetry, Cartography and Remote Sensing*, 25, 255-260.

Warchoł A. 2015. Analysis of possibilities to registration TLS point clouds without targets on the example of the Castle Bridge in Rzeszów. *International Multidisciplinary Scientific GeoConference: SGEM*; Sofia Tom 1, Surveying Geology & Mining Ecology Management (SGEM). 737-742.

Warchoł A. 2019. The concept of LiDAR data quality assessment in the context of BIM modeling, *Int. Arch. Photogramm. Remote Sens. Spatial Inf. Sci.*, XLII-1/W2, 61–66, https://doi.org/10.5194/isprs-archives-XLII-1-W2-61-2019, 2019.

Warchoł A., Balawejder M., Banaś M., Matkowska K., Nalewajek P., Wysmulski G., 2019, Measurement and Calculation of the Volume of the Heap Located in Zastawie Village in Poland, *Modern Technologies for the 3rd Millennium*, Oradea (Rumunia).

Warchoł A., Szwed P., Wężyk P. 2016. Integration of Technology of Airborne, Mobile, and Terrestrial Laser Scanning in the Process of Inventory Urban Vegetation in Selected Parts of Kraków. *In Proceedings of the Pokrycie Terenu i Przewietrzanie Krakowa*, Krakow, Poland, 20 October 2016, 67–79.

Weidner L., Walton G. 2021. Monitoring the Effects of Slope Hazard Mitigation and Weather on Rockfall along a Colorado Highway Using Terrestrial Laser Scanning. *Remote Sensing*; 13(22):4584. https://doi.org/10.3390/rs13224584.

Wolski B., Cienciała A., Hajdukiewicz M., Romanyszyn I., Krawczyk K., Gapys E., Warchoł A., Lęcznar J., Kapusta Ł., Granek G., Sobura Sz., Kulesza Ł., Zięba W., Borek K., Nawrot A., Mączyńska A., Cisek S., 2022. *Pozyskiwanie danych geodezyjnych dla potrzeb*

gospodarowania przestrzenią regionu świętokrzyskiego. Wydawnictwo Politechniki Świętokrzyskiej.

Zapłata R., Bakuła K., Stereńczak K., Kurczyński Z., Kraszewski B., Ostrowski W. 2018. Zalecenia odnośnie do pozyskiwania, przetwarzania, analizy i wykorzystania danych LiDAR w celu rozpoznania zasobów dziedzictwa archeologicznego w ramach programu AZP – między teorią a praktyką. *Kurier Konserwatorski*, 95–103.

Yang B., Li J., 2022. A hierarchical approach for refining point cloud quality of a low cost UAV LiDAR system in the urban environment. *ISPRS Journal of Photogrammetry and Remote Sensing*, 183, 403-421, https://doi.org/10.1016/j.isprsjprs.2021.11.022.

Zhao L., Ma X., Xiang Z., Zhang S., Hu C., Zhou Y., Chen G. 2022. Landslide Deformation Extraction from Terrestrial Laser Scanning Data with Weighted Least Squares Regularization Iteration Solution. *Remote Sensing*; 14(12), 2897. https://doi.org/10.3390/rs14122897.

WYKORZYSTANIE RÓŻNYCH TECHNOLOGII POMIAROWYCH DO OBLICZENIA OBJĘTOŚCI OBIEKTU SKALNEGO W REZERWACIE WIETRZNIA W KIELCACH

SŁOWA KLUCZOWE: obliczenie objętość, obiekt skalny, metoda GNSS-RTK, skanowanie laserowe, LiDAR, poziom odniesienia

STRESZCZENIE: W pracy przedstawiono procedurę pomiaru objętości nietypowego obiektu o nieregularnym kształcie jakim jest formacja skalna zlokalizowana na terenie Rezerwatu Wietrznia w Kielcach. Zastosowano dwie techniki pomiarowe: GNSS-RTK oraz naziemne skanowanie laserowe. Zastosowanie niezależnych technologii pomiarowych pozwoliło na porównanie otrzymanych wyników. Uzyskane rezultaty skłaniają do dyskusji na temat wpływu gęstości punktów pomiarowych na jakość uzyskanych wyników. Na podstawie wykonanych pomiarów możliwa jest również ocena pracochłonności zastosowanych rozwiązań.

Details of authors:

dr inż. Artur Warchoł
e-mail: awarchol@tu.kielce.pl

dr inż. Łukasz Kapusta
e-mail: kapusta@tu.kielce.pl

mgr inż. Karolina Cieciora

inż. Filip Grzyb

inż. Marcin Walski

Submitted 01.12.2023
Accepted 31.12.2023